Observation of Noise and Dissipation Effects on Dynamical Localization

B. G. Klappauf, W. H. Oskay, D. A. Steck, and M. G. Raizen
Department of Physics, The University of Texas at Austin, Austin, Texas 78712-1081
(Received 17 March 1998)

We observe the effects of noise and dissipation on dynamical localization. Our system consists of cold cesium atoms in a pulsed standing wave of light, and is an experimental realization of the δ-kicked rotor. We compare the effects of amplitude noise with those of spontaneous scattering. The experimental signature in both cases is an increased growth in energy, with qualitatively similar momentum distributions. [S0031-9007(98)06761-1]

PACS numbers: 32.80.Pj, 42.50.Vk

The role of noise and dissipation in quantum evolution has become an important area of study in recent years. The destruction of quantum interference, referred to as decoherence, is thought to be responsible for the classical nature of the macroscopic world [1]. Decoherence in the context of quantum chaos is particularly intriguing, because it exposes subtle questions about the correspondence limit, and so this topic has been the focus of much theoretical work [2–6]. On the experimental side, the effects of nonzero temperature on conductance fluctuations in mesoscopic structures [7] and the effects of noise on ionization of Rydberg atoms in microwave fields [8,9] have been studied. Nevertheless, there remain many open questions, and new experiments on decoherence in quantum chaos are clearly needed. In particular, it is important to compare the effects of controlled noise and dissipation on the *same system*, because, although noise and dissipation are fundamentally different in nature, they can have qualitatively similar effects on a quantum system.

In our earlier work with sodium atoms, we observed dynamical localization in atomic momentum transfer [10,11]. This effect is a quantum suppression of classical chaos and should be susceptible to noise or dissipation. The signature of decoherence in this system is the destruction of localization, with subsequent diffusive growth in momentum. Early efforts to observe this effect in sodium were hampered by the presence of a boundary that limited the chaotic region of the momentum space. The boundary arises from the nonzero pulse duration of the interaction Hamiltonian [11]. Over the last two years we have constructed a new experiment with cesium atoms. The larger mass and longer wavelength of the atomic transition greatly reduce the problem of the boundary [12]. These developments have led to experiments on the effects of noise and dissipation that are reported in this Letter.

To describe our system, we begin with a two-level atom with transition frequency ω_0 interacting with a pulsed standing wave of near-resonant light of frequency ω_L. For sufficiently large detuning $\delta_L = \omega_0 - \omega_L$, the excited state amplitude can be adiabatically eliminated [13]. The atom can then be treated as a point particle. In this approximation, the center-of-mass motion of the atom is described by the Hamiltonian

$$H = \frac{p^2}{2M} + V_0 \cos(2k_L x) \sum_{n=1}^{N} F(t - nT). \qquad (1)$$

Here $V_0 = \hbar\Omega^2/8\delta_L$, k_L is the wave number, T is the pulse period, Ω is the resonant Rabi frequency, and $F(t)$ is a square pulse centered at $t = 0$ with duration t_p. We can rewrite (1) as a scaled, dimensionless Hamiltonian:

$$H' = \frac{\rho^2}{2} - k \cos(\phi) \sum_{n=1}^{N} f(\tau - n), \qquad (2)$$

where $\phi = 2k_L x$, $\rho = (2k_L T/M)p$, $\tau = t/T$, $f(\tau)$ is a pulse of unit amplitude and scaled duration $\alpha = t_p/T$, $k = (8V_0/\hbar)\omega_r T^2$ is the scaled kick amplitude, $\omega_r = \hbar k_L^2/2M$ is the recoil frequency, and $H' = (4k_L^2 T^2/M)H$. In the quantized model, ϕ and ρ are conjugate variables satisfying the commutation relation $[\phi, \rho] = i\bar{k}$, where $\bar{k} = 8\omega_r T$ is a scaled Planck constant.

This system is an experimental realization of the δ-kicked rotor, an important paradigm for classical and quantum chaos [11]. The stochasticity parameter K completely specifies the classical δ-kicked rotor dynamics. For $K \gtrsim 1$, the classical dynamics are globally chaotic. For $K > 4$, the primary resonances become unstable, and the phase space is predominantly chaotic. In our system, the effective stochasticity parameter at zero momentum is given by the square-pulse expression $K = \alpha k$. The nonzero pulse widths lead to a reduction of K with increasing momentum [12].

We now consider two important modifications of this interaction. The first is to replace the fixed kick amplitude k with a random, step-dependent kick amplitude k_n, to introduce amplitude noise in the kicks. The second change is to add a weak, resonant interaction that will induce a small number of spontaneous scattering events, primarily between kicks. The latter change introduces dissipation into the system.

The experimental setup is similar to that of our earlier quantum chaos experiments in sodium [11]. The experiments are performed on laser-cooled cesium atoms in a magneto-optic trap (MOT) [14]. Two actively locked

single-mode diode lasers (L1, L2) at 852 nm are used for cooling, trapping, and detection of the cesium atoms. The main beam from L1 is double passed through a tunable acousto-optic modulator (AOM1) that provides fast control over the intensity and detuning of the beam. During the trapping stage of the experiment, the light from L1 is locked 15 MHz to the red of the $(6S_{1/2}, F = 4) \rightarrow (6P_{3/2}, F = 5)$ cycling transition. This light is collimated with a waist of 1.4 cm and has a typical power of 23 mW at the chamber. The light from L1 is split into three beams that are retroreflected through the center of the chamber in a standard six-beam MOT configuration. The second laser, L2, prevents optical pumping into the $F = 3$ ground state during the trapping and detection stages.

After trapping and initial cooling, the intensity of L1 is reduced for 1 ms and the detuning is increased to 39 MHz to further cool the sample. Typically, we trap 10^6 atoms with $\sigma_x = 0.1$ mm and $\sigma_p/2\hbar k_L = 4$. The trapping fields are then turned off, and the interaction potential is turned on. The pulsed standing wave is provided by a stabilized single-mode Ti:sapphire laser (L3). The light from L3 passes through an acousto-optic modulator (AOM2) that controls the pulse sequence. The linearly polarized beam is spatially filtered, aligned with the atoms, and retroreflected through the chamber to form a standing wave. The beam has a typical power of 290 mW at the chamber and a waist of 1.44 mm. For all of the experiments described here we detune this beam 6.1 GHz to the red of the cycling transition, with typical fluctuations of about 100 MHz. The pulse sequence consists of a series of 283 ns (FWHM) pulses with a rise/fall time of 75 ns and less than 3 ns variation in the pulse duration. The period was 20 μs with less than 4 ns variation. The detection of momentum is accomplished by letting the atoms drift in the dark for a controlled duration (typically 15 ms). The trapping beams are then turned on in zero magnetic field, forming an optical molasses that freezes the position of the atoms [10]. The atomic position is recorded via fluorescence imaging in a short (10 ms) exposure on a cooled CCD. The final spatial distribution and the free-drift time enable the determination of the one-dimensional momentum distribution. The systematic uncertainties in the determination of the momentum distributions include the spatial calibration of the imaging system and the ambiguity in the drift time due to motion occurring during different interaction times, giving an overall systematic uncertainty of $\pm 4\%$ in the momentum measurements.

We introduce amplitude noise with random pulse intensities k_n, which have a uniform distribution on an interval centered about the zero-noise intensity level. The width of this interval represents the amount of amplitude noise and is given as a percent of this mean level. To introduce dissipation, a small amount of near-resonant (molasses) light from L1, still detuned by 39 MHz, is leaked into the chamber by AOM1 during the interaction with the pulsed light. We calculated photon scattering rates from the measured intensities based on the assumption that the atoms are illuminated uniformly with all polarizations, so that the result is independent of how the magnetic sublevels are populated.

The pulse period for both cases was $T = 20$ μs, corresponding to $\bar{k} = 2.08$. The kick strength k was chosen to provide the best exponentially localized momentum distributions in the zero-noise case. For the amplitude noise data we used $V_0/h = 3.3$ MHz, corresponding to $K = 12.8$. For the dissipation case we used $V_0/h = 3.12$ MHz, corresponding to $K = 11.9$. The uncertainty in K is $\pm 10\%$, with the largest contributions due to the measurement of the laser beam profile and absolute power. The momentum boundary due to nonzero pulse width is a factor of 4 farther out than in our earlier sodium experiments. For the current experiments the reduction in the effective K value is only 6% out to $|p/2\hbar k_L| = 40$ and 25% at our maximum detectable momentum of $|p/2\hbar k_L| = 80$.

We first consider the momentum evolution with no added noise or dissipation, shown in Fig. 1(a). The initial distribution is nearly Gaussian; however, there is a pedestal that represents approximately 6% of the atoms. The distribution is also shown at later times, where it takes on an exponential profile. This characteristic behavior is a hallmark of dynamical localization [15].

The corresponding growth of energy as a function of time is shown in Fig. 2. It is important to note that the calculation of the energy, $\langle p^2 \rangle/2$, from a distribution is highly sensitive to the behavior at large p. For this reason we exclude from the calculation any points below a chosen cutoff, representing the noise floor that dominates at high momenta. Our cutoff level is at 0.25% of the peak value, representing a 400:1 signal-to-noise ratio. We checked the validity of our $\langle p^2 \rangle$ calculation by comparing it to the $\langle p^2 \rangle$ of an exponential fit to our localized distributions. These values typically agree to within 5%.

Although the distribution in Fig. 1(a) is exponential, we find that, as the kicks continue, the sides start to "bulge out." This growth, also seen in the energy, may be due to a variety of systematic noise sources in the experiment, such as the inherent amplitude noise (about 2% peak-to-peak), the spontaneous scattering from each kick ($\lesssim 0.3\%$), and inherent phase noise, which we measured to be less than 200 mrad rms over the interaction time, with a typical fluctuation period of 2 ms or longer. For our operating parameters, effects due to the fluctuating dipole force [16] and atom-atom collisions are negligible.

The effects of external noise and dissipation are shown in Figs. 1(b) and 1(c). In Fig. 1(b), noise in the kick amplitude was imposed, with a peak-to-peak deviation of 62.5% about the mean. In Fig. 1(c), the probability of spontaneous scattering was 13% per kick, with an absolute uncertainty of 20%. Both cases exhibit clear deviations from the exponential form.

Figure 2(a) displays the growth of energy as a function of time for different noise levels. The data plotted here

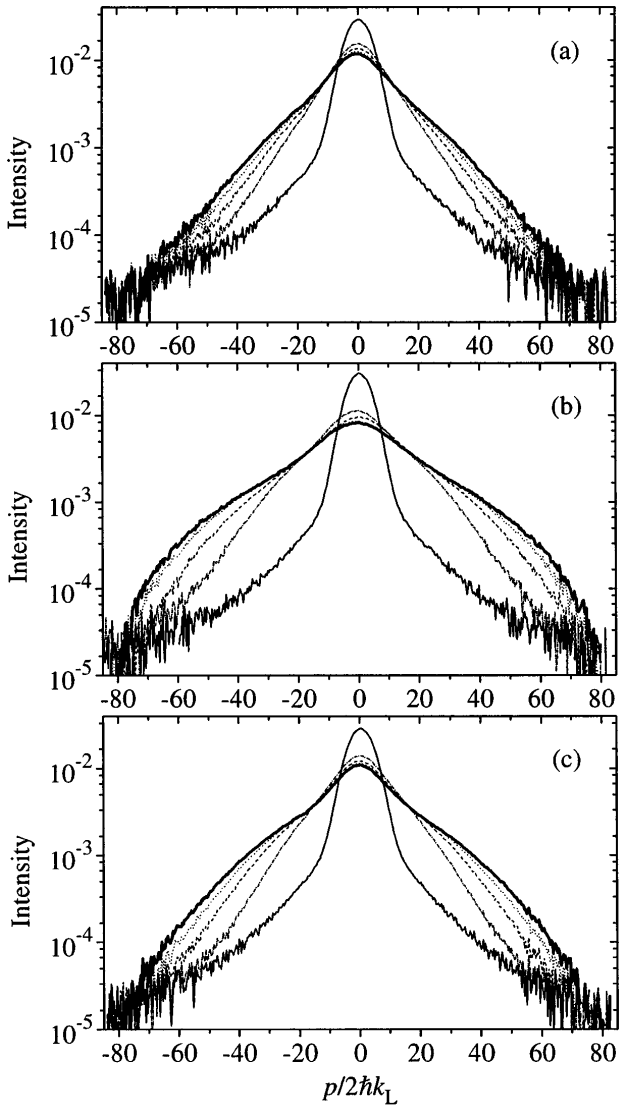

FIG. 1. Comparison of the momentum distribution evolution for the cases of (a) no noise, (b) 62.5% amplitude noise, and (c) dissipation from 13%/kick spontaneous scattering probability. Time steps shown are 0 kicks (light solid line), 17 kicks (dash-dotted), 34 kicks (dashed), 51 kicks (dotted), and 68 kicks (heavy solid) for (a) and (c), and 0, 16, 32, 52, and 68 kicks, respectively, for (b). The vertical scale is logarithmic and in arbitrary units.

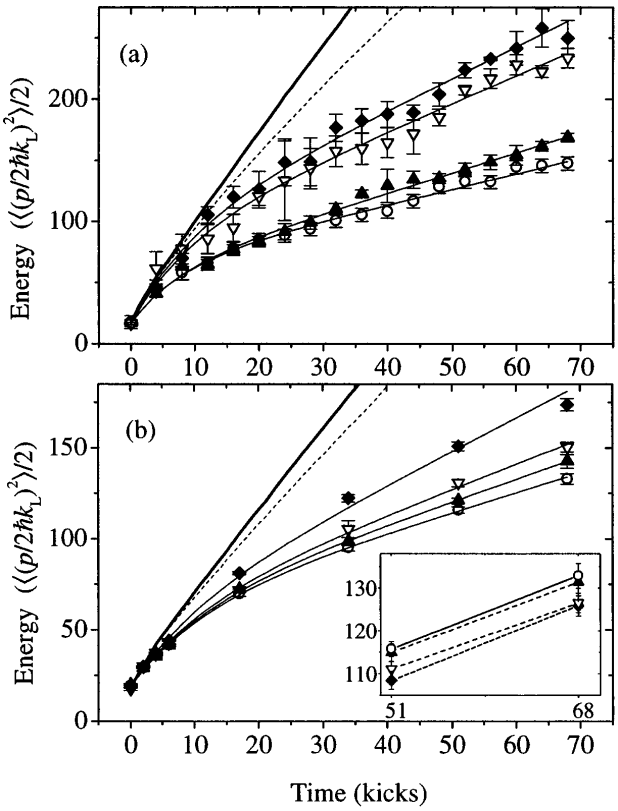

FIG. 2. Energy vs time plots for increasing amounts of amplitude noise (a) and spontaneous scattering probability (b). The values for (a) are 0%, 25%, 50%, and 62.5% noise (circles, filled triangles, open triangles, and diamonds, respectively). The values for (b) are 0%, 1.2%, 5.0%, and 13% per kick (circles, filled triangles, open triangles, and diamonds, respectively), corresponding to total intensities of 0, 27, 94, and 246 μW/cm^2. Error bars indicate a statistical uncertainty of 1 standard deviation, but do not account for the $\pm 8\%$ systematic uncertainty in the measured energy. Solid lines are curve fits using the model (3). Also shown are classical simulations of the δ-kicked rotor (heavy solid line) and the square-pulse kicked rotor (dashed) corresponding to the fit parameters. Inset shows the cooling effect when the molasses beams are added *after* the interaction time (same symbols); the solid line indicates the reference case of no added interaction.

represent an average over four distinct random kick sequences. Figure 2(b) displays the growth of energy as a function of time for different levels of spontaneous scattering. To quantify the growth of energy, we analyzed the data in Fig. 2 by employing a diffusion model suggested by Cohen [17]:

$$D(t) = D_0 \tau \left[\frac{1}{t_c} + \frac{1}{t^*} \exp\left(-\frac{t}{\tau} \right) \right], \qquad (3)$$

where $\tau^{-1} = t_c^{-1} + t^{*-1}$, and fit the data to $E(t) = \int_0^t D(t')\, dt'$. In this model, D_0 is the initial diffusion rate, t^* is the characteristic time for quantum effects to set in, and t_c is the coherence time of the noise [5]. We take D_0 and $\ln t_c$ as our fitting parameters, and we make the ansatz $D_0 = t^* \beta^{-1}$, where β is an additional fitting parameter constrained to be the same among the four simultaneous fits to the data sets in each of Figs. 2(a) and 2(b). The initial energy in each fit was constrained to be the average of the zero-kick measurements, which was 16.6 for the amplitude noise data and 19.1 for the spontaneous scattering data. The results of our fits to the data are shown in Table I. Note that the fits for $D_0(K) = D_{cl}[K \sin(\bar{k}/2)/(\bar{k}/2)]$ [5,18] give $K = 13.8$ and 12.9 for the amplitude noise and spontaneous scattering data, respectively. Here, we have used $D_{cl}(K) \simeq (K^2/2)[1/2 - J_2(K) + J_2^2(K)]$ [19], where J_2 is an ordinary Bessel function. These values for K are within the

TABLE I. Fit results for the data presented in Fig. 2. Note that the fitting errors were typically around 5% in the first case, and were around 2% in the second case. However, these fitting errors do not include the systematic uncertainties discussed in the text.

Amplitude noise			Spontaneous scattering		
Noise level	D_0	$\ln t_c$	Probability	D_0	$\ln t_c$
0%	6.98	3.78	0%	4.61	3.91
25%	7.00	3.45	1.2%	4.70	3.79
50%	9.14	3.65	5.0%	4.82	3.69
62.5%	9.70	3.62	13%	5.19	3.45
$\beta = 1.40$			$\beta = 3.32$		

uncertainty of those determined from the experimental parameters. Also, the fitted values of D_0 are relatively insensitive to the noise level, and the coherence time t_c decreases with increasing noise, except for the two largest amplitude noise cases. In these cases the fitted values for D_0 are anomalously high compared to the case with no noise, and the coherence times are longer than in the 25% case, indicating a breakdown of the fits for large amplitude noise levels.

In order to claim that the increased diffusion for the case of spontaneous scattering is due to decoherence, it is essential to characterize the role of recoil heating, which could also lead to momentum diffusion. To address this question experimentally, we measured the effect of turning on the molasses beams *after* the kick sequence instead of during the kick sequence. This measurement was repeated at each level of spontaneous scattering for the same durations as the kick sequences. The results are displayed as an inset of Fig. 2(b). We find that the molasses beams produce a weak *cooling* effect that is substantially smaller than the growth seen when they are concurrent with the kicks. Hence, our observations provide clear experimental evidence for decoherence.

The theoretical predictions regarding decoherence in the kicked rotor have so far been limited to the growth of energy and have not considered the momentum distributions. The common feature for noise and dissipation is that our observed distributions are neither simple Gaussians nor exponentially localized. The central region forms a "bubble" that is distinct from the tails. For the case of amplitude noise, these momentum line shapes agree qualitatively with a numerical simulation [20]. The case of dissipation is more complicated, and a realistic simulation has not yet been carried out.

In summary, we have observed the destruction of dynamical localization due to noise and dissipation. We hope that this work will stimulate the development of theoretical models to describe the momentum distributions.

This work was supported by the R. A. Welch Foundation and the NSF.

Note added.—After submission of this paper, the effects of spontaneous scattering on localization were reported by Ammann *et al.* [21].

[1] W. H. Zurek, Phys. Today, **44**, No. 10, 36 (1991).
[2] E. Ott, T. M. Antonsen, Jr., and J. D. Hanson, Phys. Rev. Lett. **53**, 2187 (1984).
[3] T. Dittrich and R. Graham, Europhys. Lett. **4**, 263 (1987).
[4] S. Fishman and D. L. Shepelyansky, Europhys. Lett. **16**, 643 (1991).
[5] Doron Cohen, Phys. Rev. A **44**, 2292 (1991).
[6] S. Dyrting and G. J. Milburn, Phys. Rev. A **51**, 3136 (1995).
[7] R. M. Clarke, I. H. Chan, C. M. Marcus, C. I. Duruöz, J. S. Harris, Jr., K. Campman, and A. C. Gossard, Phys. Rev. B **52**, 2656 (1995).
[8] M. Arndt, A. Buchleitner, R. N. Mantegna, and H. Walther, Phys. Rev. Lett. **67**, 2435 (1991).
[9] L. Sirko, M. R. W. Bellermann, A. Haffmans, P. M. Koch, and D. Richards, Phys. Rev. Lett. **71**, 2895 (1993).
[10] F. L. Moore, J. C. Robinson, C. Bharucha, P. E. Williams, and M. G. Raizen, Phys. Rev. Lett. **73**, 2974 (1994); J. C. Robinson, C. Bharucha, F. L. Moore, R. Jahnke, G. A. Georgakis, Q. Niu, M. G. Raizen, and Bala Sundaram, Phys. Rev. Lett. **74**, 3963 (1995).
[11] F. L. Moore, J. C. Robinson, C. F. Bharucha, Bala Sundaram, and M. G. Raizen, Phys. Rev. Lett. **75**, 4598 (1995).
[12] B. G. Klappauf, W. H. Oskay, D. A. Steck, and M. G. Raizen (to be published).
[13] R. Graham, M. Schlautmann, and P. Zoller, Phys. Rev. A **45**, R19 (1992).
[14] Steven Chu, Science **253**, 861 (1991).
[15] L. E. Reichl, *The Transition to Chaos in Conservative Classical Systems: Quantum Manifestations* (Springer-Verlag, Berlin, 1992).
[16] J. P. Gordon and A. Ashkin, Phys. Rev. A **21**, 1606 (1980).
[17] Doron Cohen (private communication).
[18] D. L. Shepelyansky, Physica (Amsterdam) **28D**, 103 (1987).
[19] A. B. Rechester, M. N. Rosenbluth, and R. B. White, Phys. Rev. A **23**, 2664 (1981).
[20] Bala Sundaram (private communication).
[21] H. Ammann, R. Gray, I. Shvarchuck, and N. Christensen, Phys. Rev. Lett. **80**, 4111 (1998).